

Elastic scattering of polarized protons from ${}^3\text{He}$ at 800 MeVM. Geso,¹ A. Azizi,² K. Amos,³ P. K. Deb,³ G. Igo,⁴ K. Jones,⁵ J. B. McLelland,⁶ G. Westen,⁷ R. Whitney,⁸ and C. Whitten⁴¹Department of Medical Radiations Sci-RMIT-University, Victoria 3083, Australia²Jet Proportional Laboratory, California Institute of Technology, 480 Oak Grove Drive, Pasadena, California 91109³School of Physics, University of Melbourne, Parkville, Victoria 3010, Australia⁴Physics Department, University of California at Los Angeles, 405 Hilgard Avenue, Los Angeles, California 90095⁵LANSCE-6, MS H 812, Los Alamos National Laboratory, Los Alamos, New Mexico 87545⁶P-DO, MS D434, Los Alamos National Laboratory, Los Alamos, New Mexico 87545⁷Department of Physics, California State University Hayward, Hayward, California 94542⁸Thomas Jefferson National Accelerator Facility, 12000 Jefferson Avenue, Newport News, Virginia 23606

(Received 21 May 2001; published 15 February 2002)

Cross section, analyzing power, and spin transfer observables for p - ${}^3\text{He}$ elastic scattering have been obtained using an 800-MeV polarized proton beam at the Los Alamos Meson Physics Facility (LAMPF). The results are compared with theoretical predictions for these observables using nonlocal optical potentials defined by full folding a complex nucleon-nucleon (NN) effective interaction with a ground state ${}^3\text{He}$ wave function given by a large space, shell model nuclear structure calculation. The effective NN interaction has been derived from complex NN potentials that fit the (complex) NN scattering phase shifts at 800 MeV.

DOI: 10.1103/PhysRevC.65.034005

PACS number(s): 25.40.Cm, 13.75.Cs, 24.70.+s

I. INTRODUCTION

Elastic scattering using the polarized proton as a probe has been extensively studied over the years not only to extract information about the spin dependence of the nuclear force but also to test the validity of various theoretical models of nuclear structure and of reactions. As part of such a general investigation, the three-nucleon systems, ${}^3\text{H}$ and ${}^3\text{He}$, are important nuclei for theoretical and experimental studies. The prediction of the properties for the three-body nuclear system represents a challenging test for existing theoretical models, many of which are based on various types of three-body nuclear forces, that have been developed over the years [1]. However, recently the shell model approach [2] has been considered with such light mass systems and very good results for the structures have been obtained when large basis spaces and NN G -matrix elements have been used. That has been so with proton scattering data analysis as well [3].

There have been a limited number of measurements of the cross section and the analyzing power for p - ${}^3\text{He}$ elastic scattering over the range of proton energies from 100 to 1700 MeV [4]. The experimental data reported in this paper represents the first measurement of the cross section and analyzing power for p - ${}^3\text{He}$ at 800 MeV. Also we report the measurement of all of the Wolfenstein spin parameters for this reaction. Since Wolfenstein spin parameters (spin observables) are sensitive to the spin dependent part of the interaction, one hopes that measurements of these observables will be helpful in better understanding the spin dependence of the nuclear forces.

It is now possible to predict observables from elastic proton-nucleus (p - A) scattering at energies from 40 to 800 MeV [3,5,6] in a manner consistent with that employed for electron scattering. This has been accomplished by solving the inhomogeneous partial wave Schrödinger equations specified with complex, nonlocal, and energy dependent optical potentials formed by full folding effective NN interac-

tions with nuclear one-body density matrix elements (OB-DME). To make predictions of p - A scattering with this approach, three basis aspects of the system under investigation must be specified. First, the description of the nucleus should be determined from a large scale structure calculation that well describes the ground state properties. The second ingredient is the single particle (SP) (bound state) wave functions. Sensible OB-DME and SP functions are those that well reproduce the longitudinal form factors measured in electron scattering. The final ingredient is the effective NN interaction that is a complex function of energy and density, describing the interaction between the incident and struck nucleons. The entire process leading to the complex nonlocal optical potentials is termed g folding; and details are given in a recent review [7].

To make such predictions for p - ${}^3\text{He}$ scattering we have used the computer codes, DWBA98 and DWBB98 of Raynal [8]. The major code DWBA98 is based upon optical potentials defined in coordinate space and so the effective interaction must be cast as a sum of central tensor and two-body spin-orbit components each having a radial variation that is a sum of Yukawa functions. Analysis of scattering data using this program have always been reported for targets ranging in mass from 3 to 238 at energies of 65 and 200 MeV [5], as well as for the energy regime extensively studied with ${}^{12}\text{C}$ [6], 40 to 800 MeV. The high quality of the results necessitated that this effective interaction be defined so that it reproduces accurately the (momentum space) half-off-shell NN t and g matrices on which it is based; the latter reflecting medium modifications due to Pauli blocking and the mean nuclear field within which the pair interact. Note that with p - ${}^3\text{He}$ elastic scattering, there are contributions from angular momentum transfer (I) values of 0 and 1. The set with $I=0$ define the nonlocal optical potential. The $I=1$ contributions are small [3] but are included in all the present results as in Ref. [3] by using the distorted wave Born approximation.

For incident energies above the pion threshold elastic scattering may still be described by optical potentials. It has been suggested [9] that these potentials be formed by folding relativistic density dependent effective interactions (Lorentz invariant amplitudes) with relativistic nuclear structure wave functions. However, based upon the success obtained using the full folding (nonrelativistic scattering) model to analyze elastic scattering of 65 and 200-MeV protons from targets ranging from ${}^3\text{He}$ to ${}^{238}\text{U}$ [5] and also now for p - ${}^{12}\text{C}$ scattering from 40 to 800 MeV [6], we consider herein just what may be achieved with that approach in analyses of 800-MeV p - ${}^3\text{He}$ scattering allowing minimal relativity. The process has been used [3] with some success to analyze p - ${}^3\text{He}$ scattering data taken with 200 and 300 MeV incident proton energies. Thus we have analyzed the present data using the same structure for ${}^3\text{He}$ used in that study [3]. In particular the OBDME have been taken from a $(0+2+4)\eta\omega$ shell model calculation for the He isotopes [2]. Note that in all the calculations leading to the results displayed, harmonic oscillator (HO) SP wave functions as set by the shell model calculations have been used.

In this paper, a complete set of data are presented for p - ${}^3\text{He}$ elastic scattering including the cross section, the analyzing power, and the spin transfer observables at 800-MeV incident proton energy. The experimental data are both tabulated (Tables I and II) and shown in figures (Fig. 1 and 2) wherein they are compared with theoretical predictions.

II. EXPERIMENTAL DETAILS

A detailed discussion of the experimental setup and the data acquisition procedures can be found in Ref. [10] and the references cited therein. These p - ${}^3\text{He}$ elastic scattering data were obtained using the high resolution spectrometer (HRS) at the Clinton Anderson Los Alamos meson physics facility (LAMPF). The 800-MeV polarized proton beam was obtained from the LAMPF linear accelerator. The proton beam polarization was measured upstream of the target by a polarimeter [11] that measured the n (normal to the scattering plane) and s (side to the beam direction) components of beam polarization simultaneously. The magnitude of the proton beam polarization was determined by the quench method [12] for the case where the beam was polarized in the l (longitudinal) direction.

The liquid helium target, constructed at the high energy physics laboratory at Stanford University, was lent by the University of Virginia. Three target cells, liquid ${}^3\text{He}$; superfluid ${}^4\text{He}$, and an empty cell to measure backgrounds, were centered in an aluminum cylinder 6 ft high and 2 ft in diameter. The operation and characteristics of this target setup is discussed in detail by Meyer [13]. The thickness of the ${}^3\text{He}$ target cell was 1.318 ± 0.015 cm corresponding to a target thickness of 0.102 ± 0.001 g/cm² at the measured pressure and temperature of the superfluid ${}^3\text{He}$. The target cell has aluminum windows, but large kinematic shifts easily separate the elastic scattering peaks of ${}^{27}\text{Al}$ and ${}^3\text{He}$ even down to the laboratory angle of 5° . The contribution of the proton-aluminum inelastic scattering is quite small in the region of the elastic p - ${}^3\text{He}$ peak. It was not possible to measure the

absolute cross section for the p - ${}^3\text{He}$ elastic scattering directly with this experimental setup. However, absolute p - ${}^3\text{He}$ elastic scattering cross sections were obtained from measurements of the relative cross sections for the p - ${}^3\text{He}$ and p - p elastic scattering using a 0.148 ± 0.005 -g/cm² CH_2 target and absolute cross sections for p - p elastic scattering taken from the Arndt phase shift program [14].

In the HRS facilities the scattered protons were focused by a quadrupole magnet through a 2×2 in.² acceptance into a configuration of two dipole magnets (the HRS) that bent the protons upwards by around 150° towards a array of detectors that both defined focal plane and acted as a proton polarimeter. The front array of detectors (drift chambers and scintillators) determined the identities and trajectories of particles at the exit of the HRS. These particles were then rescattered by a carbon analyzer of known analyzing power, and the new trajectories of these identified particles were then measured by a back array of drift chambers. The operation of the focal plane polarimeter and the extraction of the scattered beam polarization and spin dependent scattering observables is discussed in detail by McClelland *et al.* [15]. The whole HRS system of quadrupole magnets—two dipole magnets—and focal plane polarimeter was movable horizontally so that these spin dependent observables could be studied at different scattering angles.

The errors in the determination of the absolute p - ${}^3\text{He}$ elastic scattering cross sections are dominated by the 6.9% error in the normalization factor used to convert an absolute p - p elastic scattering cross section to an absolute p - ${}^3\text{He}$ absolute elastic scattering cross section. This error includes contributions from the CH_2 target thickness 3.4%, the p - p elastic scattering cross section 2.4%, the p - p analyzing power 6.1%, and the p - p elastic scattering was measured with a polarized beam locked in one normal orientation. The errors in the measured p - ${}^3\text{He}$ analyzing powers are mainly statistical but include a 1% systematic error from the proton beam polarization. The errors in the measured spin transfer observables are also mainly statistical but include uncertainties in the beam polarization and p - ${}^3\text{He}$ analyzing power. Most false asymmetries from the focal plane polarimeter are canceled to first order when the spin transfer observables are calculated from the difference between normal and reverse beam polarizations. The measured spin transfer observables do not include a systematic error, estimated to be 0.05, from the uncertainty in the analyzing power of the focal plane analyzer [23].

III. THEORETICAL DETAILS

For sometime now the structure of ${}^3\text{H}$ and ${}^3\text{He}$ have been one of the successes of few body physics and of Faddeev approach in particular. However, it is instructive to consider a shell model description of such light mass nuclei as this approach offers an alternate means to investigate the correlations in the wave functions that are naturally contained in the few body schemes. To be relevant this description must give the basic static and reaction properties of the mass 3 nuclei in reasonable if not in good agreement with observed

TABLE I. Cross section and analyzing power for p - ^3He elastic scattering at 800 MeV.

$-t$ (GeV/c) ²	θ_{lab} (deg)	$d\sigma/dt$ [mk/(GeV/c) ²]	$A_y \pm \Delta A_y$	$-t$ (GeV/c) ²	θ_{lab} (deg)	$d\sigma/dt$ [mk/(GeV/c) ²]	$A_y \pm \Delta A_y$
0.013	4.5	373.36±44	0.278±0.008	0.262	20.6	0.2468±0.02	0.047±0.013
0.016	4.9	342.03±40	0.305±0.009	0.265	20.7	0.2487±0.02	0.068±0.011
0.018	5.2	313.74±37	0.321±0.009	0.274	21.0	0.2478±0.02	0.146±0.011
0.020	5.6	285.26±34	0.323±0.010	0.282	21.4	0.2440±0.02	0.220±0.011
0.023	5.9	260.49±31	0.343±0.012	0.291	21.7	0.2468±0.02	0.301±0.011
0.037	7.5	181.22±18	0.386±0.008	0.300	22.1	0.2468±0.02	0.351±0.011
0.040	7.9	161.85±16	0.415±0.009	0.309	22.4	0.2573±0.02	0.406±0.010
0.044	8.2	149.04±15	0.407±0.009	0.321	22.9	0.2658±0.02	0.480±0.010
0.047	8.6	132.05±13	0.417±0.010	0.330	23.2	0.2658±0.02	0.477±0.010
0.051	8.9	115.62±12	0.426±0.010	0.339	23.6	0.2753±0.02	0.507±0.010
0.071	10.5	54.015±4.4	0.437±0.008	0.349	23.9	0.2724±0.02	0.510±0.010
0.076	10.9	47.370±4.0	0.429±0.008	0.362	24.4	0.2563±0.02	0.547±0.010
0.081	11.2	41.674±3.4	0.452±0.009	0.371	24.7	0.2705±0.02	0.556±0.010
0.086	11.6	36.263±3.0	0.454±0.010	0.381	25.1	0.2801±0.02	0.569±0.009
0.091	11.9	31.232±2.6	0.437±0.010	0.391	25.4	0.2715±0.02	0.549±0.010
0.118	13.5	16.423±1.3	0.412±0.008	0.405	25.9	0.2421±0.02	0.565±0.013
0.123	13.9	13.480±1.1	0.417±0.008	0.415	26.2	0.2297±0.02	0.553±0.013
0.130	14.2	11.107±0.90	0.406±0.009	0.425	26.6	0.2193±0.017	0.560±0.013
0.136	14.6	8.7355±0.72	0.387±0.010	0.435	26.9	0.2050±0.016	0.568±0.013
0.142	14.9	6.5501±0.55	0.371±0.011	0.495	28.9	0.1699±0.013	0.524±0.014
0.166	16.2	3.1042±0.24	0.317±0.007	0.506	29.2	0.1443±0.011	0.529±0.014
0.172	16.5	2.6105±0.20	0.277±0.008	0.517	29.6	0.1414±0.011	0.512±0.014
0.179	16.9	2.0979±0.16	0.260±0.009	0.528	29.9	0.1395±0.011	0.481±0.016
0.187	17.2	1.7372±0.13	0.251±0.010	0.581	31.5	0.1044±0.008	0.489±0.016
0.194	17.6	1.3385±0.10	0.186±0.012	0.592	31.9	0.0864±0.007	0.511±0.016
0.196	17.7	1.2151±0.09	0.190±0.008	0.604	32.2	0.0769±0.006	0.467±0.016
0.204	18.0	1.0062±0.08	0.134±0.009	0.615	32.6	0.0712±0.006	0.456±0.017
0.212	18.4	0.7974±0.06	0.100±0.010	0.626	32.9	0.0683±0.006	0.447±0.018
0.219	18.7	0.6360±0.05	0.050±0.012	0.682	34.5	0.0494±0.004	0.450±0.021
0.230	19.2	0.3892±0.03	0.014±0.011	0.694	34.9	0.0456±0.004	0.450±0.021
0.238	19.5	0.3417±0.03	0.009±0.011	0.706	35.2	0.0418±0.003	0.424±0.023
0.246	19.9	0.2943±0.02	-0.023±0.012	0.718	35.6		0.396±0.024
0.254	20.2	0.2658±0.02	0.020±0.013	0.730	35.9		0.378±0.025

results. The structure studies of Nvarátil and Barrett [2] show satisfactory agreement.

The simplest shell model that may be constructed for these mass 3 nuclei is to take three nucleons in the $0s$ shell. That model, however, does not involve correlations in the ground state wave function that implicitly are included in the solutions of the Faddeev equations. Such correlations can be inherent in the shell model wave functions but only from shell model calculations made with much larger model spaces. Even so, convergence with basis size on some properties is slow. For example, from calculations of the ground state of the ^3He performed in a shell model including up to 32 $\eta\omega$ excitations [2], the binding energy is still a few percent away from the exact value given by the Faddeev solution for the specified NN interaction. However, the binding energy reflects the large distance properties of the ground state wave function. On the other hand, for the momentum transfer values usually involved, most scattering processes are sensitive to details of the wave functions within the body of the

nucleus. Hence, the interest is in using a large space shell model wave function calculations of the elastic scattering of electrons and protons from ^3He . Recently [3] wave functions for the ground states of ^3He and ^4He were defined within a complete $(0+2+4)$ $\eta\omega$ shell model using the G -matrix interaction of Zheng *et al.* [16]. The shell model code OXBASH [17] was used to obtain those wave functions; and the wave function of the ground state of ^3He is segmented as

$$|\Psi(^3\text{He})\rangle = 90.21\% |0\hbar\omega\rangle + 2.39\% |2\hbar\omega\rangle + 7.40\% |4\hbar\omega\rangle.$$

The lack of convergence in the binding energies with this wave function is demonstrated in the strength of the $4\hbar\omega$ component relative to that of the $2\hbar\omega$ one. But the essential aspect is that this wave function well describes the matter properties of the ^3He ground state measured by electron elastic scattering and, at lower energies, proton elastic scattering [3].

TABLE II. The spin transfer observables for p - ^3He elastic scattering at 800 MeV.

$-t$ (GeV/c) ²	D_{ss}	$-D_{sl}$	D_{ll}	D_{ls}	D_{nn}
0.016	0.972 ± 0.025	0.074 ± 0.035	0.897 ± 0.033	0.098 ± 0.023	0.961 ± 0.036
0.041	0.891 ± 0.020	0.150 ± 0.028	0.817 ± 0.029	0.191 ± 0.020	1.015 ± 0.032
0.078	0.859 ± 0.022	0.230 ± 0.031	0.780 ± 0.029	0.271 ± 0.029	1.026 ± 0.033
0.125	0.872 ± 0.022	0.336 ± 0.029	0.771 ± 0.028	0.390 ± 0.021	0.987 ± 0.033
0.183	0.843 ± 0.026	0.545 ± 0.033	0.742 ± 0.028	0.485 ± 0.021	0.978 ± 0.034
0.250	0.507 ± 0.036	0.534 ± 0.044	0.524 ± 0.044	0.598 ± 0.036	0.965 ± 0.041
0.287	0.262 ± 0.038	0.559 ± 0.046	0.228 ± 0.044	0.586 ± 0.036	0.855 ± 0.058
0.326	0.369 ± 0.028	0.590 ± 0.033	0.543 ± 0.030	0.522 ± 0.029	
0.410	0.494 ± 0.027	0.573 ± 0.030		0.545 ± 0.028	
0.501	0.544 ± 0.037	0.571 ± 0.040		0.589 ± 0.028	
0.599	0.593 ± 0.028	0.583 ± 0.030	0.527 ± 0.029	0.640 ± 0.028	
0.702	0.496 ± 0.069	0.627 ± 0.071	0.582 ± 0.037	0.741 ± 0.036	

The Zheng interaction [16] has a unique property not found in the usual (phenomenological) interactions. It is defined by the G -matrix elements of a realistic NN potential that requires specification of HO SP wave functions at the outset. Thus, in principle, there are no parameters left for adjustment in making analyses of electron and proton scattering observables. The longitudinal form factor for elastic scattering of electrons found using the specified single particle wave functions [3] is almost an exact reproduction of the data, but the transverse (magnetic) form factor for electron scattering from ^3He is underpredicted by an order of magnitude. However, this magnetic form factor has a small magnitude compared to the longitudinal form factor. The proton scattering data from ^3He at 200 and 300 MeV were also analyzed in the same study [3]. Such analyses require the additional specification of the (complex and nonlocal) optical potential, which was derived from the self-same g -folding approach that we adopt herein. That description is also parameter free, and the predictions for the 200 and 300 MeV proton scattering observables agreed well with data [3].

Those results encourage credence in use of many body methods to give a quality description of ^3He within at least the central region of the nucleus, so long as the structure model is defined by a large basis space model.

A realistic microscopic model of p - A reactions is one based upon NN t matrices whose on-shell values are consistent with measured NN scattering data to and above the incident energies of interest. Below pion threshold, the phenomenology of the NN interactions is relatively simple, and several one boson exchange potential (OBEP) models [18] have been found that provide very good fits to NN phase shift data. That is not the case above pion threshold, as inelastic channels open and resonance scattering occurs. Simple potentials must be varied to account for the various meson production thresholds and also to account for effects of known [$P_{33}(1232)(\Delta)$ and $P_{11}(1440)(N^*)$] resonance structures in the NN system. There exist extensions to OBEP models that incorporate resonance and particle production [19] and with which some NN and $NN\pi$ data up to 1 GeV may be explained. The NN phase shifts above pion threshold found

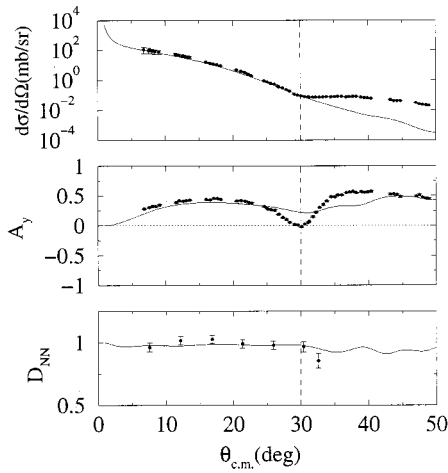


FIG. 1. The cross section $d\sigma/d\Omega$, analyzing power A_y , and the D_{nn} spin transfer observable for p - ^3He elastic scattering at 800 MeV along with the theoretical predictions.

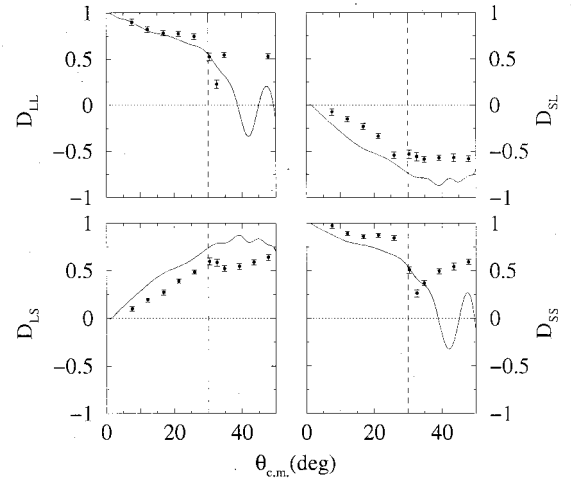


FIG. 2. The spin transfer observables D_{ll} , D_{ls} , D_{sl} , and D_{ss} for p - ^3He elastic scattering at 800 MeV along with the theoretical predictions.

with these models are better than any from standard OBEP but as yet they are not adequate in a number of important channels. However, the characteristics of the experimental NN scattering amplitudes up to 2.5 GeV are consistent with the optical potential concept. Recently [20], the SM97 data [21] has been interpreted very well by a basic OBEP supplemented by sensible complex optical potentials. With the OBEP component established by the fits its use gave with data below 300 MeV, the supplementing NN optical potentials reflected the effects of the $P_{33}(1232)$ and $P_{11}(1440)$ resonances in several partial waves. The version found using the coupled channel Bonn III (BCC3) OBEP model [18] as the basic interaction has been used in the present calculations.

Effective interactions that accurately map the associated NN t matrices on shell are then the input for the folding model of the p - A optical potentials. Also, as Ray [22] suggests, the effects of Pauli blocking may be still important at 800 MeV. We have solved the Bethe-Breuckner-Goldstone BBG equations allowing for the Pauli blocking (and for a mean field in the propagators) to define the NN G matrices for the complex NN interactions. However, we do not find there to be any substantial effects of the nuclear medium upon the effective interactions at 800 MeV. The prescription by which those effective interactions are given has been found to be appropriate at lower energies [3,5,6]. The t and g matrices have been mapped into the coordinate space forms of effective interactions, appropriate for use in the code DWBA98, to obtain solutions of the nonlocal Schrödinger equations associated with the complex nonlocal optical potentials resulting from the g -folding process.

IV. RESULTS AND DISCUSSION

The differential cross section, analyzing power, and the spin transfer observables for p - ^3He elastic scattering at 800-MeV proton incident energy are given in Tables I and II. Comparison of experimental results with the theoretical analyses made using the g -folding optical potential are presented in Figs. 1 and 2.

In Fig. 1 the differential cross section, analyzing power, and spin transfer observable D_{nn} are compared with the results found using the g -folding optical potential. Those predictions are displayed by the solid curves. The cross section and analyzing power data span a scattering angle range from 7° to 50° in the center-of-mass system, with the cross-section values from 30° onwards being of the order of 0.1 mb/sr. Dashed vertical lines are given in each plot to note where the cross section has become that small, and to indicate where our model calculation breaks down in comparison to measured values of the cross section. Indeed that is the case. This we define as the “credibility limit” of the theoretical analysis

method used, and to that angle, the predicted cross section agrees very well with the data. Small changes in calculated phase shifts as would be brought by the uncertainties in specification of the nonlocal potential as well as by what one could expect (or hope) from higher contributions will affect the results at the larger scattering angles where the scattering theory and/or the approximation inherent with its implementation are not well defined. The calculated analyzing power agrees well with the data to 25° and trends towards the minimum at 30° without reaching a null value. Over the range up to 30° the experimental data for the spin transfer observable D_{nn} is practically 1.0 and the theoretical calculations reproduce this behavior.

The other spin transfer observables, D_{ll} , D_{ls} , D_{sl} , and D_{ss} , are compared with the results of our calculations in Fig. 2. Again the theory credibility limit (at 30°) is shown in each panel by the vertical dashed lines. To that limit, the measured spin observable values are in qualitative agreement with the trend of the calculations. In particular D_{ll} is well reproduced while the calculations overpredict the measured values of both D_{ls} and D_{sl} and underpredict the measured D_{ss} values.

In summary, we have used the BCC3 boson exchange model NN interaction modulated by NN optical potentials that reproduce the SM97 NN scattering phase shifts to 2.5 GeV to specify NN t and g matrices at 800 MeV. Coordinate space effective interaction forms that map those t and g matrices have been determined and then used in a g -folding process to specify a complex and nonlocal optical potential for 800-MeV polarized protons incident on ^3He . The structure of the target nucleus used in that folding was determined from a large space shell model calculation; and the ground state wave function that leads to an electron scattering longitudinal form factor in good agreement with measured values. Thereby all quantities required in the folding process have been present, allocating solutions of the associated nonlocal p - ^3He Schrödinger equations predictive of the scattering phase shifts and so of the differential cross sections and spin transfer observables. The predicted results agree reasonably well with the observations for momentum transfer values up to where the cross section has decreased to the order of 0.1 mb sr.

ACKNOWLEDGMENTS

The authors would like to thank LAMPF for technical and financial support. This work was supported by the U.S. Department of Energy, Nuclear Physics Division under Contract Nos. DOE-AT03-81ER40027 and DERG-0588-ER40390. M.G. is grateful to the Faculty of Life Sciences-RMIT-University for travel Grant Nos. 1999 and 2000. The theoretical part of this research was supported by a research grant from the Australian Research Council.

- [1] J. L. Friar, B. F. Gibson, and G. L. Payane, *Annu. Rev. Nucl. Part. Sci.* (1984), and references therein.
 [2] P. Navrátil and B. R. Barrett, *Phys. Rev. C* **57**, 3119 (1998); (private communication).

- [3] P. J. Dortmans, K. Amos, and S. Karataglidis, *J. Phys. G* **23**, 183 (1997); P. J. Dortmans, K. Amos, S. Karataglidis, and J. Raynal, *Phys. Rev. C* **58**, 2249 (1998), and references cited therein.

- [4] N. P. Goldstein *et al.*, *Can. J. Phys.* **48**, 2696 (1970); H. Langevin-Joliot *et al.*, *Nucl. Phys.* **A158**, 309 (1970); R. Frascaria *et al.*, *Nuovo Cimento Lett* **2**, 240 (1971); *Phys. Lett.* **66B**, 329 (1977); M. Blecher *et al.*, *Phys. Rev. Lett.* **24**, 1126 (1970); J. Fain *et al.*, *Nucl. Phys.* **A262**, 413 (1976); G. D. Aklazov *et al.*, *Phys. Lett.* **85B**, 43 (1979); D. K. Hasell *et al.*, in *Conference on Nuclear Structure*, Amsterdam, 1982, edited by A. van der Woude and B. J. Verhaar (European Physical Society, Amsterdam, 1982), and references therein.
- [5] P. J. Dortmans, K. Amos, and S. Karataglidis, *J. Phys. G* **23**, 183 (1997); P. J. Dortmans, K. Amos, S. Karataglidis, and J. Raynal, *Phys. Rev. C* **58**, 2249 (1998), and references cited therein.
- [6] P. K. Deb and K. Amos, *Phys. Rev. C* **62**, 016007 (2000).
- [7] K. Amos, P. J. Dortmans, H. V. von Geramb, S. Karataglidis, and J. Raynal, *Adv. Nucl. Phys.* **25**, 275 (2000).
- [8] J. Raynal, report NEA 1205/02, 1999.
- [9] S. J. Wallace, *Annu. Rev. Nucl. Part. Sci.* **37**, 267 (1987); J. J. Kelly and S. J. Wallace, *Phys. Rev. C* **49**, 1315 (1994), and references cited therein.
- [10] A. Azizi, Ph.D. thesis, UCLA, 1985.
- [11] M. W. McNaughton, P. R. Bevington, H. R. Willard, E. Winkelmann, E. P. Champerlin, F. H. Cverna, N. S. P. King, and H. Williams, *Phys. Rev. C* **23**, 1128 (1981).
- [12] G. G. Ohlsen and P. W. Keaton, *Nucl. Instrum. Methods* **109**, 41 (1973).
- [13] H. O. Meyer, technical report LA-Ur-733, 1977.
- [14] R. Arndt (unpublished).
- [15] J. B. McClelland *et al.*, technical report LA-U-84-1671, 1984.
- [16] D. C. Zheng, B. R. Barrett, J. P. Vary, W. C. Haxton, and C.-L. Song, *Phys. Rev. C* **52**, 2488 (1995).
- [17] A. Etchegoyen, W. D. M. Rae, and N. S. Godwin, computer code OXBASH-MSU (the Oxford-Buenos-Aries-Michigan State University shell model code) MSU version by B. A. Brown, 1986; B. A. Brown, A. Etchegoyen, and W. D. M. Rae, MUSCL Report No. 524, 1986 (unpublished).
- [18] R. Machleidt, *Adv. Nucl. Phys.* **19**, 189 (1989); R. Machleidt and G. Q. Li, *Phys. Rep.* **242**, 5 (1994); L. Jäde and H. V. von Geramb, *Phys. Rev. C* **57**, 496 (1998); L. Jäde, *ibid.* **58**, 96 (1998).
- [19] Ch. Elster, W. Ferchländer, K. Holinde, D. Schütte, and R. Machleidt, *Phys. Rev. C* **37**, 1647 (1988); A. Bulla and P. U. Sauer, *Few-Body Syst.* **12**, 141 (1992), and references cited therein.
- [20] H. V. von Geramb, K. Amos, H. Läbes, and M. Sander, *Phys. Rev. C* **58**, 1948 (1998).
- [21] R. A. Arndt, C. H. Oh, I. I. Strakovsky, R. L. Workman, and F. Dohrmann, *Phys. Rev. C* **56**, 3005 (1997).
- [22] L. Ray, *Phys. Rev. C* **41**, 2816 (1990).
- [23] R. W. Ferguson *et al.*, *Phys. Rev. C* **33**, 239 (1986).